

Histone Deacetylase 8 in Neuroblastoma Tumorigenesis

Ina Oehme,¹ Hedwig E. Deubzer,^{1,5} Dennis Wegener,¹ Diana Pickert,¹ Jan-Peter Linke,¹ Barbara Hero,⁷ Annette Kopp-Schneider,² Frank Westermann,³ Scott M. Ulrich,⁸ Andreas von Deimling,^{4,6} Matthias Fischer,⁷ and Olaf Witt^{1,5}

Abstract Purpose: The effects of pan-histone deacetylase (HDAC) inhibitors on cancer cells have shown that HDACs are involved in fundamental tumor biological processes such as cell cycle control, differentiation, and apoptosis. However, because of the unselective nature of these compounds, little is known about the contribution of individual HDAC family members to tumorigenesis and progression. The purpose of this study was to evaluate the role of individual HDACs in neuroblastoma tumorigenesis.

Experimental Design: We have investigated the mRNA expression of all HDAC1-11 family members in a large cohort of primary neuroblastoma samples covering the full spectrum of the disease. HDACs associated with disease stage and survival were subsequently functionally evaluated in cell culture models.

Results: Only *HDAC8* expression was significantly correlated with advanced disease and metastasis and down-regulated in stage 4S neuroblastoma associated with spontaneous regression. High *HDAC8* expression was associated with poor prognostic markers and poor overall and event-free survival. The knockdown of HDAC8 resulted in the inhibition of proliferation, reduced clonogenic growth, cell cycle arrest, and differentiation in cultured neuroblastoma cells. The treatment of neuroblastoma cell lines as well as short-term-culture neuroblastoma cells with an HDAC8-selective small-molecule inhibitor inhibited cell proliferation and clone formation, induced differentiation, and thus reproduced the HDAC8 knockdown phenotype. Global histone 4 acetylation was not affected by HDAC8 knockdown or by selective inhibitor treatment.

Conclusions: Our data point toward an important role of HDAC8 in neuroblastoma pathogenesis and identify this HDAC family member as a specific drug target for the differentiation therapy of neuroblastoma.

The pharmacologic inhibition of histone deacetylases (HDAC) is an emerging novel molecular treatment strategy in cancer therapy (1, 2). HDAC inhibitors have been shown to induce the inhibition of proliferation, apoptosis, and clonogenic growth and to promote differentiation in several cancer cell lines *in vitro*, and to exert antitumoral effects in mouse models (3, 4). Subsequently, clinical trials are under way to evaluate the safety and efficacy of HDAC inhibitors (1). Recently, the first substance of this class, Vorinostat (suberoylanilide hydroxamic

acid), has been approved by the Food and Drug Administration for the treatment of cutaneous T-cell lymphoma⁹ (5, 6).

The human HDAC family is composed of 18 genes: *HDAC1*, *HDAC2*, *HDAC3*, and *HDAC8* (class I); *HDAC4*, *HDAC5*, *HDAC6*, *HDAC7*, *HDAC9*, and *HDAC10* (class II); *HDAC11* (class IV); and 7 sirtuins (class III; refs. 4, 7, 8). HDAC inhibitors can act through binding the active site and chelation of the catalytic zinc ion located at its base (9–11). However, because of the highly conserved nature of the enzymatic pocket,

Authors' Affiliations: ¹Clinical Cooperation Unit Pediatric Oncology, ²Department of Biostatistics, ³Department of Tumor Genetics, and ⁴Clinical Cooperation Unit Neuropathology, German Cancer Research Center; ⁵Department of Pediatric Oncology, Hematology and Immunology, University of Heidelberg; ⁶Department of Neuropathology, University Hospital of Heidelberg, Heidelberg, Germany; ⁷Department of Pediatric Oncology, University Children's Hospital of Cologne, Cologne, Germany; ⁸Department of Chemistry, Ithaca College, Ithaca, New York

Received 3/14/08; revised 6/26/08; accepted 7/22/08.

Grant support: Heinrich F.C. Behr stipend for medical students, University of Heidelberg (J.-P. Linke); Federal Ministry of Education and Research (Bundesministerium für Bildung und Forschung; National Genome Research Network or Nationalen Genomforschungsnetz) grant N2KR-S19T03 and European Embryonal Tumor Pipeline (European Union) grant 037260 (F. Westermann); Deutsche Krebshilfe grants 502719 and 106847, Federal Ministry of Education and Research (Bundesministerium für Bildung und Forschung; National Genome Research Network or Nationalen Genomforschungsnetz) grant 01GS0456, and Fördergesellschaft

Kinderkrebs-Neuroblastom-Forschung eV (M. Fischer); Deutsche Krebshilfe grants 70-443, FO-2032-Be7, and 102546 (B. Hero); Research Corporation Cottrell College Science Award grant CC5955 (S. Ulrich); and Federal Ministry of Education and Research (Bundesministerium für Bildung und Forschung; National Genome Research Network or Nationalen Genomforschungsnetz) grant 01GS0459 (O. Witt).

The costs of publication of this article were defrayed in part by the payment of page charges. This article must therefore be hereby marked *advertisement* in accordance with 18 U.S.C. Section 1734 solely to indicate this fact.

Note: Supplementary data for this article are available at Clinical Cancer Research Online (<http://clincancerres.aacrjournals.org/>).

Requests for reprints: Olaf Witt, Clinical Cooperation Unit Pediatric Oncology G340, German Cancer Research Center, Im Neuenheimer Feld 280, D-69120 Heidelberg, Germany. Phone: 49-6221-423570; Fax: 49-6221-423277; E-mail: o.witt@dkfz.de.

© 2009 American Association for Cancer Research.

doi:10.1158/1078-0432.CCR-08-0684

Translational Relevance

Histone deacetylase (HDAC) inhibitors are an emerging class of promising novel anticancer drugs. However, little is known which of the 11 classic HDAC family members is the most relevant drug target for therapy. First phase I or II trials show that the unselective inhibition of HDACs causes a variety of side effects. Therefore, identification and selective targeting of the most critical cancer-relevant HDAC family member may reduce unspecific effects and increase antitumor efficacy in the future. This work describes for the first time the clinical relevance of a particular HDAC family member, HDAC8, in a large study cohort of tumor patients using childhood neuroblastoma as a model. High HDAC8 expression correlates with established clinical and genetic risk factors, neuroblastoma progression, and the poor survival of patients. The selective targeting of HDAC8 causes the inhibition of cell proliferation and clonogenic growth and the induction of neuronal differentiation in culture models. Thus, the work opens novel antineuroblastoma treatment perspectives using selective HDAC8 small-molecule inhibitors.

most HDAC inhibitors are not able to selectively inhibit individual HDAC isoenzymes and are therefore considered as pan-inhibitors. The inhibitory profile of currently used HDAC inhibitors within the entire HDAC family is poorly defined, in part because of the difficulty of producing recombinant purified HDACs that are functionally active (4). Thus far, only few compounds have shown selectivity against individual HDACs *in vitro* (12, 13). Therefore, little is known about the contribution of single HDAC family members to proliferation, cell cycle, apoptosis, and differentiation following the treatment of cancer cells with HDAC inhibitors and their role in tumorigenesis (14, 15).

Here, we show that HDAC8 expression significantly correlates with the disease stage and outcome of neuroblastoma, a highly malignant childhood cancer derived from the sympathetic nervous system (16). Functional analysis by RNA interference shows that HDAC8 is involved in the regulation of proliferation, clonogenic growth, and neuronal differentiation of neuroblastoma cells. HDAC8-selective small-molecule inhibitor reproduces the HDAC8 knockdown phenotype. These data point toward a functional role for HDAC8 in neuroblastoma pathogenesis and identify this HDAC as a specific target for the development of differentiation therapy strategies.

Materials and Methods

Neuroblastoma samples. The expression of HDAC1, HDAC2, HDAC3, HDAC6, HDAC7, HDAC9, and HDAC11 was analyzed using oligonucleotide microarrays in 251 neuroblastomas as described previously (17). The expression of HDACs not represented on the array (HDAC4, HDAC5, HDAC8, and HDAC10) as well as HDAC2 and HDAC11 was investigated by real-time reverse transcription-PCR (RT-PCR) in a cohort of 118 samples. The neuroblastomas of these

118 patients were diagnosed between the years 1989 and 2003. All patients were enrolled in the German Neuroblastoma trials with informed consent (18, 19). Clinical stage was classified according to the International Neuroblastoma Staging System (stage 1, $n = 19$; stage 2, $n = 9$; stage 3, $n = 16$; stage 4, $n = 49$; stage 4S, $n = 25$; ref. 20), and histopathologic prognostic category grouping was done according to the Shimada classification (21, 22). MYCN was assessed in one or more central laboratories using fluorescence *in situ* hybridization, PCR, and/or Southern blot techniques (H. Christiansen, Marburg; M. Schwab, Heidelberg; R. Spitz, Cologne). Aberrations (deletion, imbalance) of chromosomes 1p and 11q were assessed by fluorescence *in situ* hybridization as outlined previously (23, 24).

Oligonucleotide microarray analysis. Microarray analysis, total RNA preparation from snap-frozen neuroblastoma samples, and data acquisition and processing were done as previously published (17). For more details, see Supplementary Data. All raw and normalized microarray data are available at the ArrayExpress database (accession: E-TABM-38).¹⁰

Real-time RT-PCR analysis of mRNA. The real-time RT-PCR analysis of mRNA expression in tumor samples and cell lines was done as previously described (25, 26). Detailed information on primer sequences and protocols are provided in the Supplementary Data.

Statistical analysis. Analysis of oligonucleotide microarray data was done using Rosetta Resolver (V5.1, Rosetta Inpharmatics LLC). The patients' subgroups of interest were compared by Benjamini-Hochberg corrected one-way ANOVA. For the comparison of expression data between different patient subgroups (1p, 11q, Shimada, MYCN, age at diagnosis), Wilcoxon rank sum test was used. ANOVA was used for comparisons in expression between disease stages. All contrasts were tested, and P values were adjusted according to Bonferroni. Kaplan-Meier estimates for survival were plotted with R [R version 2.4.1 (2006-12-18) 2006, The R Foundation for Statistical Computing, ISBN 3-900051-07-0]. Cut point analysis for overall and event-free survival was done for HDAC8 using maximally selected rank statistics as implemented in the package maxstat (27) in R. For overall survival analysis, the optimal cut point for $\Delta\Delta C_T$ values was 3.68 (maximal log-rank statistical $M = 3.575$; $P = 0.01984$). The same cut point was chosen for event-free survival (here maximal log-rank statistical $M = 3.321$; $P = 0.04771$). Five-year overall and event-free survival with confidence interval was calculated with R. For overall survival, death from any cause was counted. For event-free survival, death from any cause, relapse, progression, or second malignancy was defined as event. Cox proportional hazard model was used to investigate whether HDAC8 (dichotomized with the cut point 3.68) is a prognostic factor adjusted for the covariates 1p, 11q, Shimada, and MYCN.

To compare the small interfering RNA (siRNA) of interest with negative control siRNA, a two-tailed t test of significance was done using GraphPad Prism version 3.0a. Means are represented in bar charts, and error bars represent the SD of at least three independent experiments.

Cell lines and reagents. Human neuroblastoma cell lines BE(2)-C, SH-SY5Y, Kelly, NGP, SH-EP, WAC2, and SK-N-BE(2) were cultured under standard conditions (see Supplementary Data).

Short-term-culture neuroblastoma cells (NB2), originally isolated from the bone marrow of a patient with metastasized stage 4 neuroblastoma (MYCN amplified) after obtaining informed consent, were cultured in DMEM with L-glutamine and 4.5 g/L glucose containing 10% fetal bovine serum and 1% nonessential amino acids (28). Selective HDAC8 inhibitor (compound 2) is described elsewhere (12). The compound was dissolved in DMSO as a stock of 250 mmol/L. Pan-HDAC inhibitors trichostatin A and valproic acid were used as previously described (26). All-trans-retinoic acid (Sigma) was dissolved in ethanol as a stock of 10 mmol/L.

Transfection with siRNA. Cells (3×10^4 per well) were seeded into 6-well plates 24 h before transient transfection with 5 or 25 nmol/L

⁹ Zolinza (Vorinostat). Food and Drug Administration 2006; <http://www.fda.gov/cder/foi/label/2006/021991lbl.pdf>.

¹⁰ <http://www.ebi.ac.uk/arrayexpress>

siRNA, respectively, for 18 h using HiPerFECT according to the manufacturer's instructions (Qiagen). For HDAC8 knockdown, the following siRNAs were used: siRNA1 [ID 120597, exon 1 and 2, Ambion (Europe) Ltd.], siRNA2 (ID 2120599, exon 5, Ambion), siRNA3 (ref. 29; sense, 5'-ACGGGCCAGUAUGGUGCAUTT-3'; antisense, 5'-AUGCACCAUACUGGCCCGUTT-3'; Ambion), siRNA4 (Hs_HDAC8_5_HP, Qiagen), and siRNA5 (HDAC8 ON-TARGETplus SMARTpool, Dharmacon, Inc.). For HDAC2 knockdown, the following siRNAs were used: siRNA1 (ID 120208, exon 3, Ambion), siRNA2 (ID 213400, exon 2, Ambion), siRNA3 (ID 120209, exon 5, Ambion), and siRNA4 (ID 120210, exon 7 and 8, Ambion). As negative controls, the following siRNAs were used: NC-1 (siCONTROL RISC-Free siRNA 1, Dharmacon), NC-2 (Silencer Negative Control 1, Ambion), and NC-3 (AllStars Negative Control siRNA, Qiagen). Transfection efficacy in BE(2)-C cells was 90.3% (confidence interval, 80.5-100.2%) as determined by fluorescently labeled siRNA siGLO Lamin A/C (Dharmacon).

Overexpression of HDAC8. An expression plasmid containing the HDAC8 cDNA sequence was cloned by using the gateway (Invitrogen) cloning system (pEXP3.2-HDAC8 = pcDNA3.2/V5-DEST × pENTR221-HDAC8) and verified by DNA sequencing (GATC). BE(2)-C neuroblastoma cells were transfected with either HDAC8-containing expression plasmid or empty vector control, respectively, using Lipofectamine 2000 (Invitrogen) transfection reagent. Transfected cells were cultivated in the presence of 1 mg/mL G418. Stably transfected clones were selected, and increased HDAC8 expression was verified by real-time RT-PCR.

Western blot analysis. Western blot analysis of whole-cell extracts was done as described previously (26). Detailed information on antibodies and protocols are provided in the Supplementary Data.

Immunocytochemistry. Immunocytochemistry was done on an automated stainer (Benchmark XT, Ventana) following the protocols of the manufacturer. Sections were pretreated for 60 min (CC1 buffer, Ventana), followed by incubation with HDAC8 antibody, 1:100 dilution, for 32 min at 37°C. The binding of HDAC8 antibody was detected (ultra View Red Detection Kit v3, Ventana), followed by counterstaining with hematoxylin (Nexes Hematoxylin, 760-201, Ventana) for 4 min and by a bluing step (Nexes bluing reagent, Ventana) for 4 min.

Soft agar assay. To determine the ability of anchorage-independent growth, clonogenic assays were done as described by the manufacturer (Chemicon International). Colonies were stained with 0.005% (w/v) crystal violet. All experiments were done in triplicate, and experiments were repeated thrice.

Growth curve. Cells (3×10^4 per well) were seeded in six-well plates; transfected with siRNA; and harvested at 0, 24, 48, 72, 96, and 144 h. The number of cells was determined by automated cell counting. Experiments were done in triplicate and repeated thrice. To calculate the population doubling time, a nonlinear regression (curve fit) was done using GraphPad Prism version 3.0a.

Caspase-3-like activity assay. Caspase-3-like protease activity was determined as previously published (30). Detailed information on the protocol is provided in the Supplementary Data.

Immunofluorescence and 4',6-diamidino-2-phenylindole staining. BE(2)-C cells (3×10^4) were grown on glass slides. Six days after transfection with siRNAs, cells were fixed for 15 min in 2% (w/v) paraformaldehyde and permeabilized for 15 min with 0.1% (v/v) Triton X-100 in PBS. After washing thrice with PBS, cells were blocked [PBS-Triton with 10% goat serum and 0.25% (w/v) BSA] for 1 h at room temperature, incubated overnight with anti-NEF antibody (polyclonal rabbit, Chemicon; 1:100) at 4°C, washed with PBS, and incubated with Cy3-labeled goat anti-rabbit antibody (Dianova; 1:100) for 3 h at room temperature. For the detection of apoptosis, cells were grown for 48 h, fixed, permeabilized, and stained with 250 ng/mL 4',6-diamidino-2-phenylindole solution. Slides were analyzed with the Olympus CKX41 microscope, $\times 10$ objective lens, and ColorView I FW camera. The exposure time was 200 ms. Cell imaging software was used for the acquisition of microscopic images.

Cell cycle analysis and apoptosis detection. Cell cycle profiles and sub-G₁ areas of cells were analyzed as described previously (31, 32).

HDAC activity assay. Overall HDAC activity was measured as previously published (33). Detailed information on the protocol is provided in the Supplementary Data.

Results

High HDAC8 expression is correlated with markers of poor outcome and advanced stage disease in neuroblastoma. Neuroblastoma is characterized by a broad clinical spectrum of disease ranging from localized stage I with excellent prognosis of about 90% survival to metastatic stage 4 neuroblastoma associated with poor survival of about 30%. Furthermore, stage 4S neuroblastoma is associated with spontaneous regression in most patients, despite metastasis into liver, skin, and bone marrow (16).

We investigated the mRNA expression of all 11 non-sirtuin HDAC family members in large cohorts of primary neuroblastoma samples from the German Neuroblastoma trial using oligonucleotide microarray ($n = 251$) or real-time RT-PCR analysis ($n = 118$). The comparison of HDAC1-11 expression in stage 4 versus stage 1 disease revealed that only HDAC8 expression was significantly associated with advanced-stage disease (Supplementary Table S2).

The detailed analysis of HDAC8 expression by real-time RT-PCR in 118 neuroblastoma samples covering all clinical stages, as well as defined genetic (1p and 11q aberration and MYCN amplification) and histopathologic risk groups, is shown in Fig. 1. HDAC8 expression was low in localized stages 1 to 3 but showed significantly higher expression levels in metastasized stage 4 disease (Fig. 1A). Interestingly, expression was low in metastasized stage 4S disease, known to be associated with spontaneous regression (Fig. 1A). High HDAC8 expression levels significantly correlated with 11q (Fig. 1B) and 1p (data not shown) unfavorable cytogenetic aberrations, as well as unfavorable Shimada histopathologic classification (Fig. 1C). The Shimada histopathologic classification system groups neuroblastoma patients into a favorable or unfavorable category based on the degree of differentiation of neuroblastoma cells, the amount of intercellular stroma, the mitosis-karyorrhexis index, and the patient age (34). Finally, HDAC8 expression was significantly increased in older patients (>18 months) known to be associated with unfavorable outcome (Fig. 1D). MYCN oncogene amplification was not associated with differential HDAC8 expression (data not shown). These results clearly show that among all 11 HDAC family members, only HDAC8 expression correlates with advanced disease stage but is low in stage 4S neuroblastoma known to be associated with spontaneous regression. In addition, HDAC8 expression correlates with molecular risk factors, unfavorable histopathology, and older age.

High HDAC8 transcript levels correlate with adverse clinical outcome of neuroblastoma patients. To determine whether HDAC8 expression levels are related to differences in patients' outcome, Kaplan-Meier estimates for overall survival and event-free survival were calculated. As expected from the strong correlation with established prognostic markers, it turned out that high HDAC8 expression was associated with adverse clinical outcome (Fig. 2A and B). In neuroblastomas with high HDAC8 expression, 5-year overall survival was 25.9% (95% confidence interval, 8.7-77.1%) versus 77.8% (confidence interval, 69.9-86.5%) in tumors with low HDAC8 expression. Event-free survival was 25.9% (confidence interval, 8.7-77.1%)

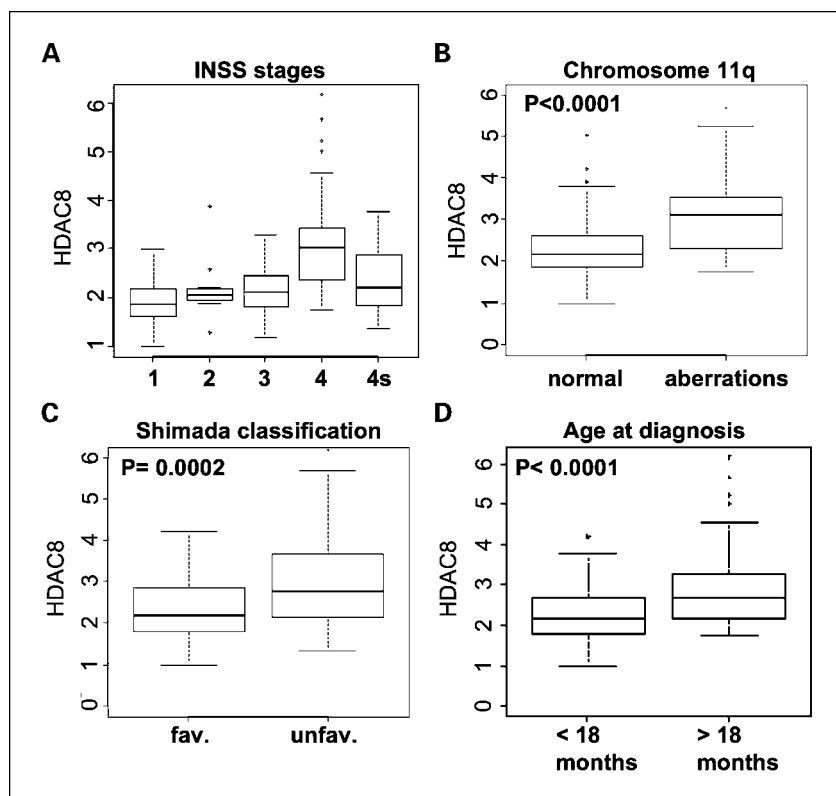


Fig. 1. *HDAC8* expression correlates with advanced-stage disease and markers of poor outcome in neuroblastoma. **A**, analysis of *HDAC8* expression in 118 neuroblastoma samples with real-time RT-PCR reveals significantly higher expression in International Neuroblastoma Staging System stage IV tumors compared with International Neuroblastoma Staging System stages 1 ($P < 0.0001$), 2 ($P = 0.0229$), 3 ($P = 0.0006$), and 4S ($P = 0.0009$). All contrasts are tested. The Y axis represents the relative *HDAC8* mRNA expression normalized against housekeeping genes (*SDHA*, *HPRT*) and calculated relatively to the lowest expression sample, which was set to 1. ANOVA analysis showed that stage has a significant effect ($P < 0.0001$). Bonferroni-adjusted comparisons between the groups showed that stages 1 and 4 differ significantly ($P < 0.0001$), stages 2 and 4 differ significantly ($P = 0.0229$), stages 3 and 4 differ significantly ($P = 0.0006$), and stages 4 and 4S differ significantly ($P = 0.0009$). **B**, high *HDAC8* expression significantly correlates with chromosome 11q ($P < 0.0001$). **C**, high *HDAC8* expression significantly correlates with unfavorable Shimada histopathologic classification ($P = 0.0002$). Fav, favorable; unfav, unfavorable Shimada classification. **D**, *HDAC8* expression significantly correlates with patient's age at diagnosis. Patients older than 18 mo express higher levels of *HDAC8* ($P < 0.0001$). For comparison of expression data between different patient subgroups (**B-D**), Wilcoxon rank sum test was used.

versus 73.8% (confidence interval, 65.6-83.1%), respectively. For comparison, we have calculated survival curves of the investigated patient cohort according to the *MYCN* oncogene amplification status, which is an established genetic marker for neuroblastoma risk stratification (Fig. 2C and D).

Cox regression revealed that *HDAC8* expression was not an independent factor for overall or event-free survival when covariates 1p aberration, 11q aberration, Shimada classification, and *MYCN* were included in the analysis.

Taken together, these results show that *HDAC8* transcript levels discriminate neuroblastoma patients with benign and adverse outcome.

Knockdown of *HDAC8* inhibits cell proliferation and clonogenic growth of neuroblastoma cells. To investigate the functional role of *HDAC8* in a cell culture model, we analyzed its expression in neuroblastoma cell lines BE(2)-C, SK-N-BE(2), NGP, Kelly, WAC2, SH-EP, SH-SY5Y, and IMR32. All cells revealed detectable *HDAC8* expression at the mRNA level. In addition, we did a Western blot analysis of several neuroblastoma cell lines and primary tumor samples confirming *HDAC8* protein expression in all samples investigated (Supplementary Fig. S1). Immunohistochemistry of selected neuroblastoma samples revealed variable *HDAC8* protein expression with a predominant cytoplasmic staining pattern (Supplementary Fig. S1).

We selected BE(2)-C cells for further experiments because these cells (a) form colonies in soft agar, (b) possess stem cell-like characteristics with the potential to recapitulate many aspects of neuroblastoma biology (35), and (c) respond to pharmacologic HDAC inhibition with reduced proliferation and the induction of neuronal differentiation and apoptosis (32). We reduced endogenous *HDAC8* expression by transiently

transfecting siRNAs into BE(2)-C cells. Three different control siRNAs and five different siRNAs targeting various parts of the *HDAC8* mRNA sequence were used to control for unspecific as well as off-target effects. The efficient reduction of mRNA and protein levels was obtained lasting at least 96 h (Supplementary Fig. S2).

The transfection of all *HDAC8* siRNAs caused a reduction of cell proliferation compared with control transfections (Fig. 3A). The calculation of the population doubling time from estimated growth curves revealed a twice higher doubling time for *HDAC8* siRNA1-transfected BE(2)-C (50 h) cells compared with negative control-transfected cells (26 h, data not shown). To investigate the role of *HDAC8* for anchorage-independent clonal growth capability, we did soft agar assays after transfection of BE(2)-C cells with siRNAs. Again, all siRNAs directed against *HDAC8* produced similar results, causing a significant reduction in colony numbers compared with control transfections (Fig. 3B).

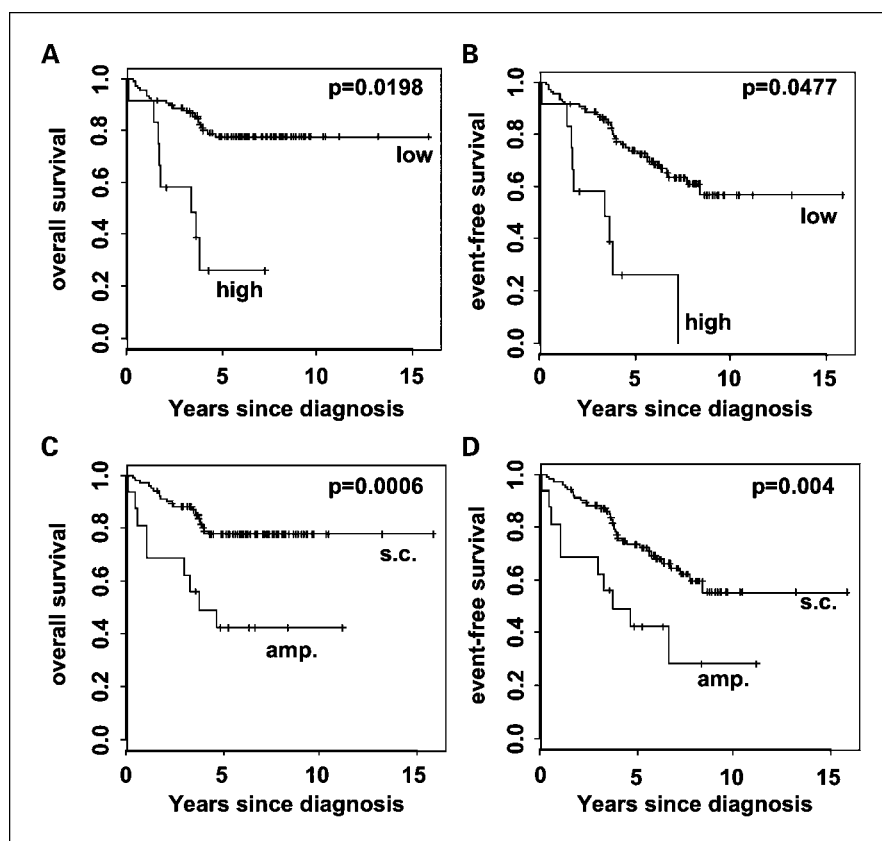
***HDAC8* controls differentiation.** *HDAC8* knockdown induced morphologic changes indicative of neuronal differentiation such as outgrowth of neurite-like structures (Fig. 4A; *HDAC8* siRNA1 and siRNA2). Knockdown of *HDAC2*, which served as a specificity control, resulted in fragmented, detached cells, suggestive of apoptosis (Fig. 4A; *HDAC2* siRNA1 and siRNA2). Neurite-like extensions occurring after *HDAC8* knockdown stained positive for neurofilament (Fig. 4B). To further characterize the morphologic changes induced by *HDAC8* knockdown, we analyzed the expression of a panel of neuronal differentiation marker genes. All investigated markers were up-regulated following *HDAC8* knockdown using a representative siRNA (Fig. 5A). At the same time, nestin, a marker for undifferentiated neuronal precursor cells, was

down-regulated (Fig. 5A). These changes could not be observed following HDAC2 knockdown of cells (data not shown). We confirmed the expression of the differentiation marker neurotrophin receptor kinase A (NTRK1/TrkA) at the protein level using Western blot analysis (Fig. 5B). Because the differentiation of cells is typically associated with a cell cycle arrest, we analyzed cell cycle distribution following HDAC8 knockdown. Indeed, we could observe a G₀/G₁ arrest with 85 ± 3% of cells transfected with HDAC8 siRNA1 in G₀/G₁ compared with 67 ± 5% negative control (NC-2)-transfected cells in G₀/G₁ ($P < 0.0001$; Fig. 5C), associated with induction of p21^{WAF1/CIP1} mRNA (Fig. 5D) and protein (data not shown), which is known to mediate cell cycle arrest in response to pharmacologic HDAC inhibition (36). The apoptotic phenotype observed following HDAC2 knockdown (Fig. 4A) was confirmed by a significant increase in caspase-3-like activity, nuclear condensation, and amount of cells in the sub-G₁ area of the cell cycle profile (Supplementary Fig. S3). In contrast, HDAC8 knockdown did not affect the apoptosis rates (Supplementary Fig. S3). Similar results were obtained in Kelly, SH-EP, and SK-N-BE(2) neuroblastoma cells, showing the induction of differentiation markers following HDAC8 knockdown (Supplementary Fig. S4). The overexpression of HDAC8 resulted in the suppression of neurofilament and NTRK1 neurotrophin receptor expression. Furthermore, retinoic acid-induced morphologic differentiation was inhibited by HDAC8 overexpression (Supplementary Fig. S5).

Thus, HDAC8 knockdown initiates a differentiation program, whereas HDAC2 knockdown induces apoptosis in neuroblastoma cells.

HDAC8-selective small-molecule inhibitor as a potential compound for the differentiation therapy of neuroblastoma. The knockdown experiments suggest that specific targeting of HDAC8 may be a novel rationale for the differentiation therapy of neuroblastoma. Recently, HDAC8-selective inhibitors were designed based on linkerless hydroxamic acids (12). These compounds show IC₅₀ for HDAC8, which was >100-fold lower compared with other class I and II HDACs (12). Treatment with the HDAC8-selective inhibitor compound 2 at concentrations in the range of its *in vitro* IC₅₀ against HDAC8 resulted in reduced cell density and outgrowth of neurite-like structures (Fig. 6A) that stained positive for neurofilament (Fig. 6B). Cell proliferation was inhibited in a concentration-dependent manner in three neuroblastoma cell lines. In addition, treatment of short-term-culture primary neuroblastoma cells derived from the bone marrow of a patient with metastasized disease with compound 2 revealed the inhibition of proliferation (Fig. 6C), which was associated with the induction of p21^{WAF1/CIP1} and NTRK1/TrkA gene expression (data not shown). The influence of compound 2 on clonogenic growth was tested in BE(2)-C cells, which are able to grow anchorage independently. The HDAC8-selective inhibitor reduced the formation of clones in soft-agar concentration dependently (Fig. 6D). The HDAC8-selective nature of compound 2 is supported by the observation that the treatment of cells increased neither global histone H4 nor tubulin acetylation, which are substrates for HDAC1/2 and HDAC6, respectively (2, 13, 37). Furthermore, total intracellular HDAC activity was not reduced by compound 2 in contrast to the pan-HDAC inhibitors valproic acid and trichostatin A (Supplementary Fig. S6).

Fig. 2. HDAC8 expression correlates with poor survival in neuroblastoma. Kaplan-Meier survival curves of overall (A) and event-free (B) survival. Low HDAC8 expression correlates with favorable overall ($P = 0.0198$) and event-free ($P = 0.0477$) survival, whereas high HDAC8 expression correlates with poor outcome. Cut point analysis for overall and event-free survival was done for HDAC8 using maximally selected rank statistics. The optimal cut point was $\Delta\Delta C_T$ value 3.68 for overall survival as well as event-free survival. $\Delta\Delta C_T$ values above this cut point were considered as high HDAC8 expression, whereas lower values were considered as low HDAC8 expression. For comparison, survival curves according to MYCN amplification status in the investigated patient cohort are shown in C (overall survival) and D (event-free survival). s.c., single copy; amp., amplified.



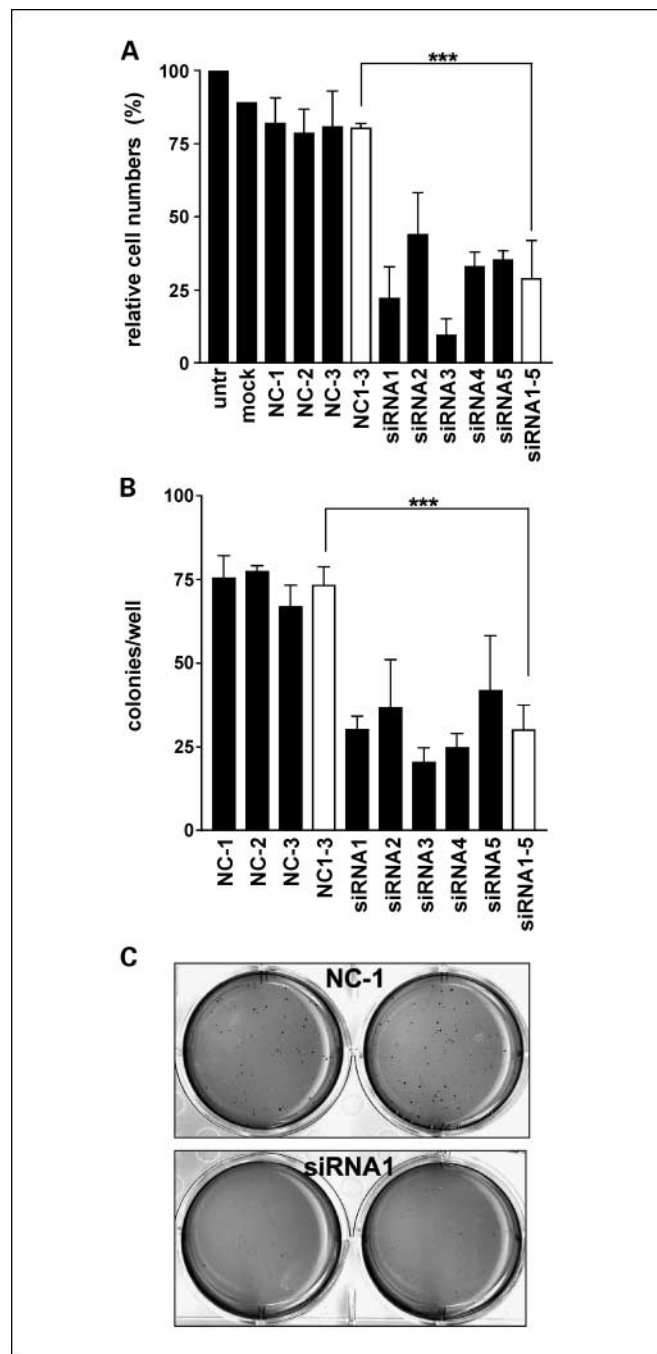


Fig. 3. HDAC8 knockdown decreases BE(2)-C cell growth. *A*, HDAC8 knockdown results in significantly decreased cell numbers using five different siRNAs (*black columns*; siRNA1-5) and is additionally depicted as mean value (*open column*; siRNA1-5; mean = $29 \pm 13\%$; $P = 0.0011$) compared with three negative control siRNAs (*open column*; NC1-3; mean = $80 \pm 2\%$). Cell numbers are expressed relative to untreated cells. *B*, HDAC8 knockdown results in significant lower amounts of colonies formed in soft agar with five different siRNAs (*black columns*) and is additionally depicted as mean value (*open column*; siRNA1-5; mean = 30 ± 8 colonies per well; $P = 0.0005$) compared with three negative control siRNAs (*open column*; NC1-3; mean = 73 ± 6 colonies per well). *C*, grown colonies stained with crystal violet from negative control siRNA (NC-1, *top*) and HDAC8 siRNA1 (*bottom*) – transfected BE(2)-C cells.

In conclusion, a HDAC8-selective small-molecule inhibitor reproduces the differentiation phenotype induced by RNA interference-mediated HDAC8 knockdown in established as well as short-term-culture primary neuroblastoma cells.

Discussion

Despite the broad application of HDAC inhibitors in preclinical models and their recent introduction in clinical trials, little is known about the cancer relevance of individual

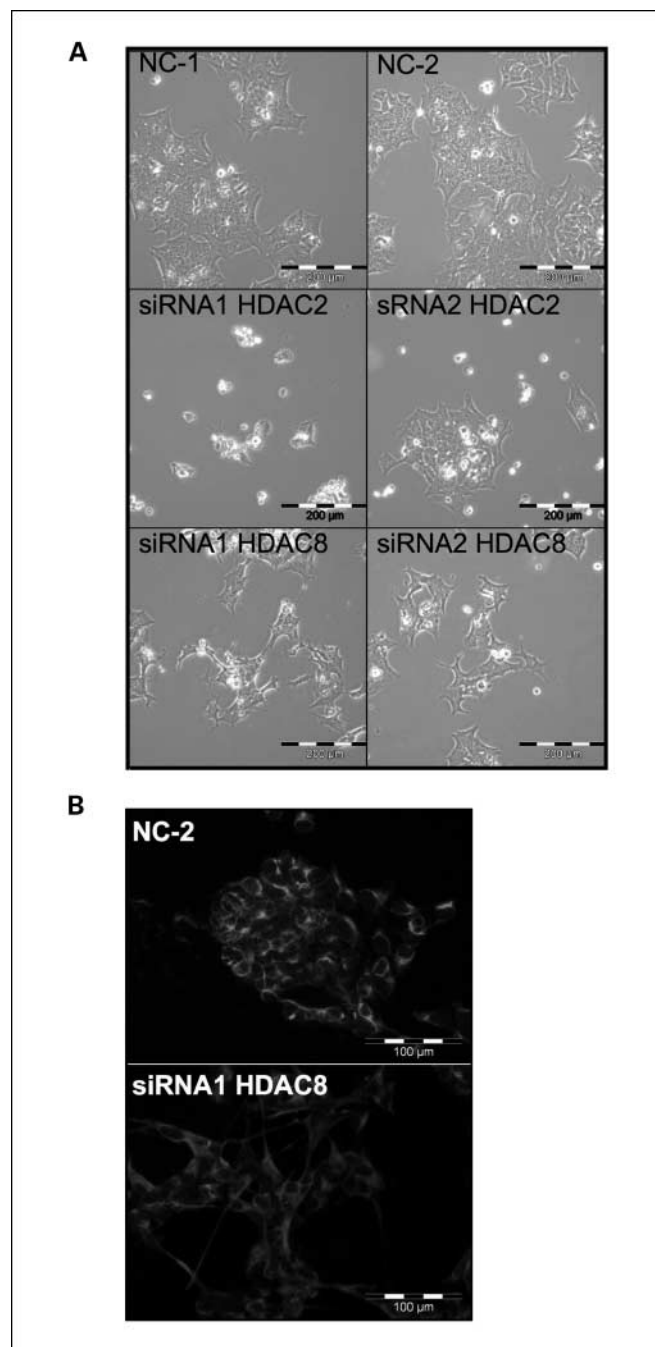
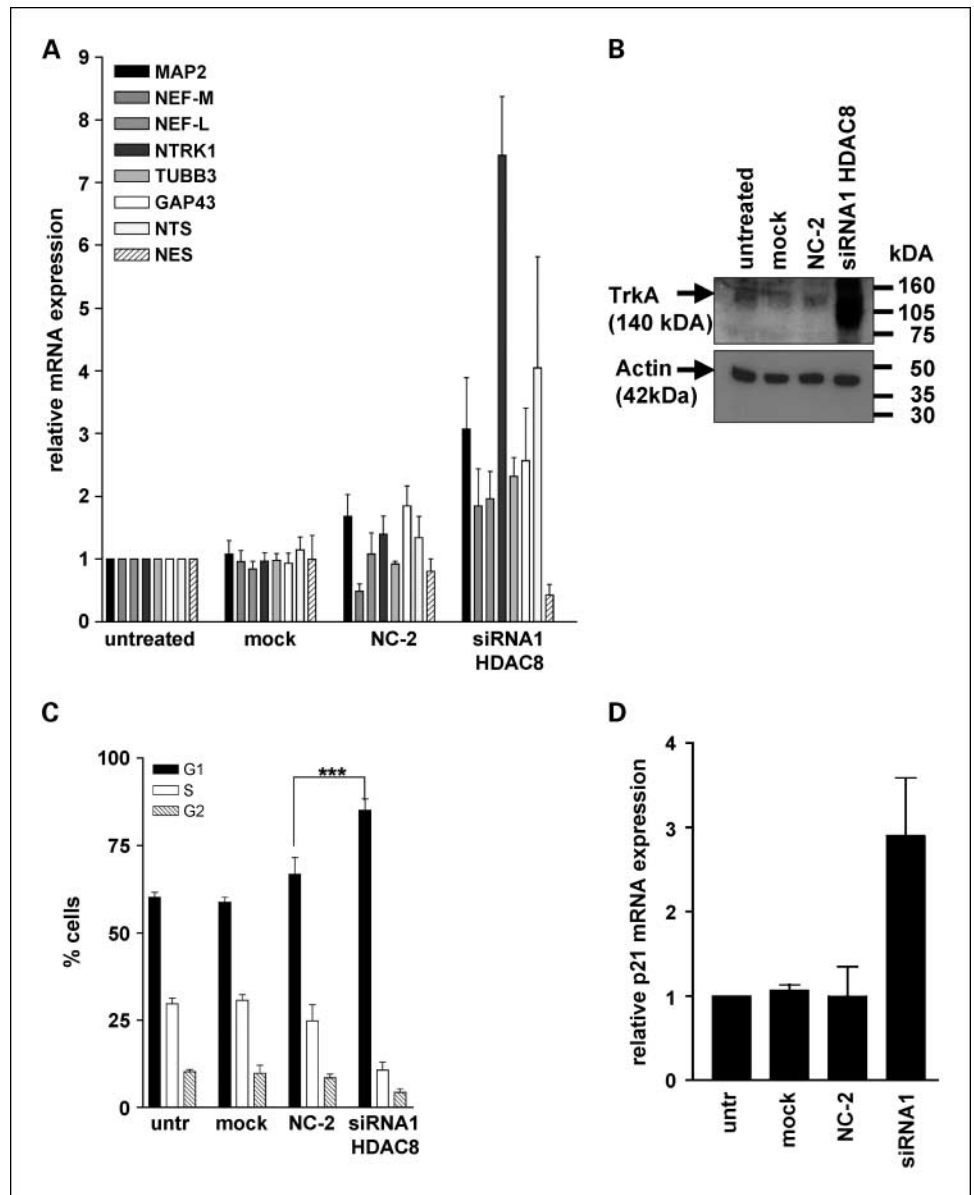


Fig. 4. HDAC8 knockdown induces a neuronal phenotype in BE(2)-C cells. *A*, HDAC8 knockdown induces outgrowth of neurite-like structures in BE(2)-C cells using different siRNAs (HDAC8 siRNA 1 and 2), whereas HDAC2 knockdown increases the amount of rounded, shrunken, and detached cells suggestive of cell death (HDAC2 siRNA 1 and 2). NC-1-2, cells transfected with negative control siRNAs 1 and 2. *B*, neurofilament staining of neurite-like structures occurring after HDAC8 knockdown using an antibody recognizing NEF-M. Top, cells transfected with negative control siRNA2 (NC-2). Bottom, cells transfected with siRNA1 targeting HDAC8.

Fig. 5. HDAC8 knockdown induces differentiation of BE(2)-C cells. **A**, transfection with siRNA (siRNA1) directed against HDAC8 induces expression of differentiation markers (*MAP2*, *NEF-M*, *NEF-L*, *NTRK1*, *TUBB3*, *GAP43*, *NTS*) and reduction of nestin (*NES*), a marker for undifferentiated neural progenitor cells. Mock, cells treated with transfection reagent only; NC-2, cells transfected with negative control siRNA2. **B**, NTRK1 expression is confirmed on protein level with an antibody recognizing Trk (140 kDa). **C**, analysis of cell cycle profile reveals that HDAC8 knockdown assembles 85% cells in G₀/G₁ (black column), 11% in S (open column), and 4% in G₂/M (hatched column), whereas transfection with NC-2 siRNA distributes 67% of cells in G₀/G₁, 25% of cells in S, and 8% of cells in G₂/M phase of the cell cycle. The difference in G₀/G₁ is significant ($P < 0.0001$). **D**, the G₀/G₁ arrest induced by HDAC8 siRNA1 is associated with *p21*^{WAF1/CIP1} mRNA up-regulation.



HDAC family members. This lack of information is mainly due to the broad inhibitory activity of the commonly used HDAC compounds, making it impossible to define the responsible HDAC controlling cell proliferation, apoptosis, and differentiation. However, the identification of the cancer-relevant HDAC family members would allow the design of selective inhibitors and facilitate insights into the molecular mechanism of biological programs suppressed in cancer cells.

Based on the following observations, we propose that HDAC8 is involved in neuroblastoma pathogenesis and provides a novel specific drug target for differentiation therapy of neuroblastoma. (a) *HDAC8* expression is up-regulated in advanced stage and metastasized disease and is associated with poor prognostic markers such as 1p and 11q aberration, age, and unfavorable Shimada histopathologic classification. (b) *HDAC8* expression is down-regulated in stage 4S neuroblastoma known to be associated with spontaneous regression. (c) High expression correlates with poor overall survival and event-

free survival of patients. (d) The knockdown of HDAC8 causes the inhibition of proliferation, reduction of clonogenic growth, and induction of cell cycle arrest and differentiation of neuroblastoma cells. Conversely, *HDAC8* overexpression suppressed the endogenous expression of differentiation markers and inhibited retinoic acid-induced morphologic differentiation. (e) The treatment of neuroblastoma cells with a HDAC8-selective small-molecule inhibitor reproduced the phenotype obtained with siRNA-mediated knockdown of HDAC8 in established as well as short-term-culture neuroblastoma cells.

Little is known about the function of HDAC8. Expression analysis suggest a role in differentiation of smooth muscle cells (38). Proliferation of lung, colon, and cervical cancer cell lines is reduced after HDAC8 knockdown (39), and, recently, HDAC8 has been implicated in the regulation of telomerase activity (40).

Thus far, there are no systematic data available on the expression of HDAC1 to HDAC11 family members in a large patient cohort. Our data show for the first time that only

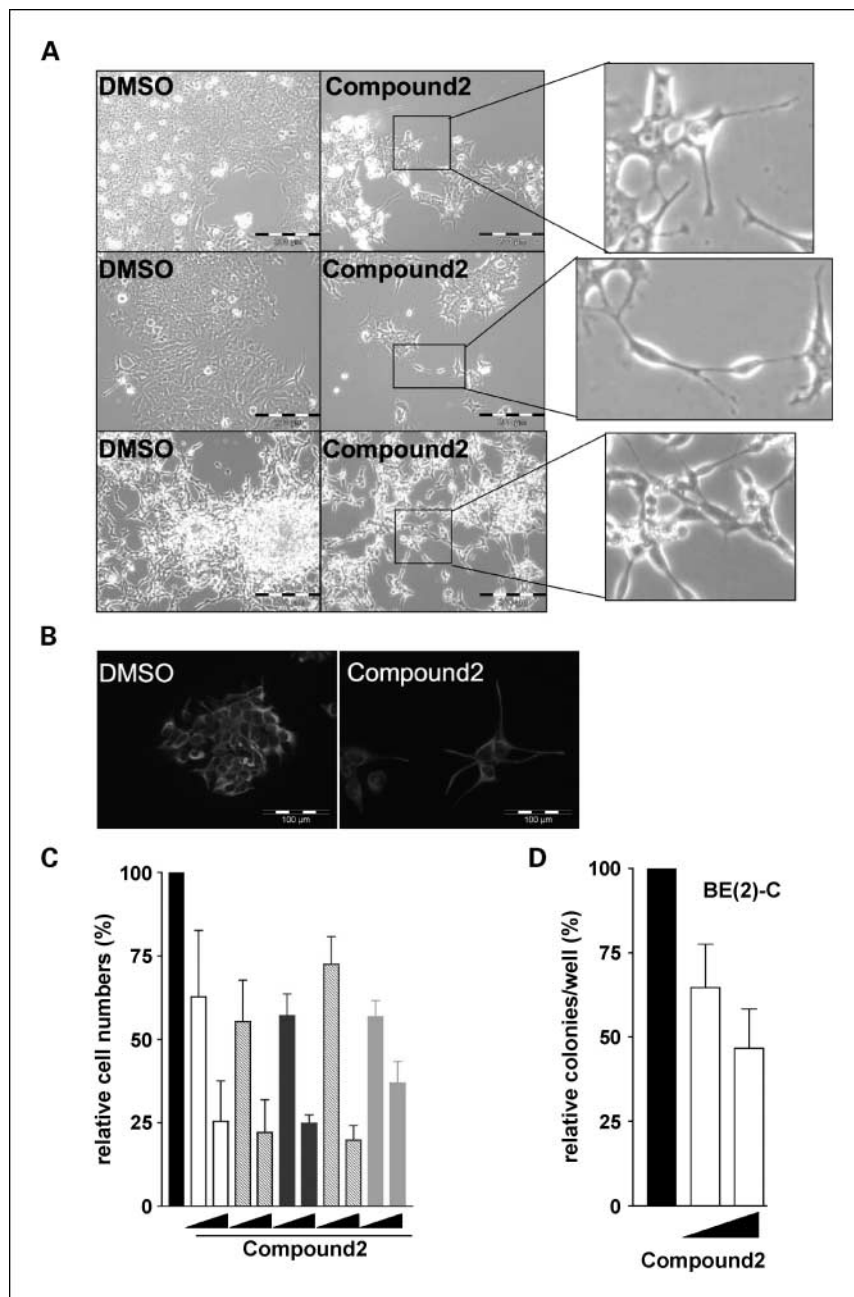


Fig. 6. HDAC8-selective compound reproduces HDAC8 knockdown phenotype in cell lines and in short-term-cultured neuroblastoma cells. *A*, treatment of BE(2)-C cells (*top*; 20 $\mu\text{mol/L}$ compound 2), SK-N-BE(2) cells (*middle*; 10 $\mu\text{mol/L}$ compound 2), and short-term-culture neuroblastoma cells (*bottom*, 40 $\mu\text{mol/L}$ compound 2) with a selective HDAC8 inhibitor (compound 2) decreases the amount of cells and induces outgrowth of neurite-like structures. *B*, incubation of SK-N-BE(2) cells with compound 2 (20 $\mu\text{mol/L}$) leads to increased NEF protein expression (immunostaining) in neurite outgrowths. *C*, treatment of BE(2)-C (*columns 2 and 3*) and SK-N-BE(2) (*columns 4 and 5*) with 10 and 20 $\mu\text{mol/L}$ as well as Kelly (*columns 6 and 7*) and SH-SY5Y (*columns 8 and 9*) with 20 and 40 $\mu\text{mol/L}$ compound 2 reduces cell numbers in a concentration-dependent manner. Short-term-culture neuroblastoma cells treated with compound 2 (20 and 40 $\mu\text{mol/L}$) are depicted as columns 10 and 11. Cell numbers are expressed relative to DMSO-treated control cells (*column 1*); the arrow is the increasing concentration of compound 2. *D*, treatment of cells with compound 2 (10 and 20 $\mu\text{mol/L}$; *open columns*) reduces the ability of BE(2)-C cells for anchorage-independent growth. Colony numbers are expressed relative to DMSO-treated control cells (*black column*).

HDAC8 expression significantly correlates with disease stage and progression in a large cohort of cancer patients. HDAC1 (41–43), HDAC2 (14, 15), and HDAC3 (42) have been found to be expressed at higher levels in cancer tissues in small numbers of selected clinical samples. Interestingly, HDAC1 has recently been found to be up-regulated in chemotherapy resistant neuroblastoma cells *in vitro* (44). Thus, the up-regulation of members of the class I HDAC family members seem to be a common theme in tumor biology.

By directly comparing the phenotype of HDAC8 and HDAC2 knockdown, we found that these family members control different cellular programs, that is, HDAC8 down-regulation releases a differentiation program whereas HDAC2 knockdown causes apoptosis. This may explain the different biological effects observed with pan-HDAC inhibitors on

cancer cells. Interestingly, global histone acetylation, a widely used surrogate marker for intracellular HDAC inhibition, was not increased, and global HDAC enzymatic activity within cells was not changed following HDAC8 knockdown in contrast to HDAC2 knockdown, supporting the HDAC8-selective targeting approach in our culture models.

Taken together, our findings point toward an important role of HDAC8 in neuroblastoma pathogenesis and highlight this HDAC family member as a novel drug target for differentiation therapy.

Note Added in Proof

Recently, a novel HDAC8-selective compound, PCI-34051, was described (Balasubramanian et al. Leukemia 2008;22:

1026–34). The compound induces apoptosis in T-cell lymphoma or leukemia cell lines but not in cells derived from solid tumors, suggesting a tumor type–selective activity.

Disclosure of Potential Conflicts of Interest

No potential conflicts of interest were disclosed.

References

1. Yoo CB, Jones PA. Epigenetic therapy of cancer: past, present and future. *Nat Rev Drug Discov* 2006; 5:37–50.
2. Minucci S, Pelicci PG. Histone deacetylase inhibitors and the promise of epigenetic (and more) treatments for cancer. *Nat Rev Cancer* 2006;6:38–51.
3. Marks P, Rifkind RA, Richon VM, Breslow R, Miller T, Kelly WK. Histone deacetylases and cancer: causes and therapies. *Nat Rev Cancer* 2001;1:194–202.
4. Bolden JE, Peart MJ, Johnstone RW. Anticancer activities of histone deacetylase inhibitors. *Nat Rev Drug Discov* 2006;5:769–84.
5. Kelly WK, O'Connor OA, Marks PA. Histone deacetylase inhibitors: from target to clinical trials. *Expert Opin Investig Drugs* 2002;11:1695–713.
6. Kelly WK, O'Connor OA, Krug LM, et al. Phase I study of an oral histone deacetylase inhibitor, suberoylanilide hydroxamic acid, in patients with advanced cancer. *J Clin Oncol* 2005;23:3923–31.
7. de Ruijter AJ, van Gennip AH, Caron HN, Kemp S, van Kuilenburg AB. Histone deacetylases (HDACs): characterization of the classical HDAC family. *Biochem J* 2003;370:737–49.
8. Gao L, Cueto MA, Asselbergs F, Atadja P. Cloning and functional characterization of HDAC11, a novel member of the human histone deacetylase family. *J Biol Chem* 2002;277:25748–55.
9. Finnin MS, Donigian JR, Cohen A, et al. Structures of a histone deacetylase homologue bound to the TSA and SAHA inhibitors. *Nature* 1999;401:188–93.
10. Nielsen TK, Hildmann C, Dickmanns A, Schwienhorst A, Ficner R. Crystal structure of a bacterial class 2 histone deacetylase homologue. *J Mol Biol* 2005; 354:107–20.
11. Sternson SM, Wong JC, Grozinger CM, Schreiber SL. Synthesis of 7200 small molecules based on a substructural analysis of the histone deacetylase inhibitors trichostatin and trapoxin. *Org Lett* 2001;3: 4239–42.
12. Krennhrubec K, Marshall BL, Hedglin M, Verdin E, Ulrich SM. Design and evaluation of "Linkerless" hydroxamic acids as selective HDAC8 inhibitors. *Bioorg Med Chem Lett* 2007;17:2874–8.
13. Haggarty SJ, Koeller KM, Wong JC, Grozinger CM, Schreiber SL. Domain-selective small-molecule inhibitor of histone deacetylase 6 (HDAC6)-mediated tubulin deacetylation. *Proc Natl Acad Sci U S A* 2003; 100:4389–94.
14. Zhu P, Martin E, Mengwasser J, Schlag P, Janssen KP, Gottlicher M. Induction of HDAC2 expression upon loss of APC in colorectal tumorigenesis. *Cancer Cell* 2004;5:455–63.
15. Huang BH, Laban M, Leung CH, et al. Inhibition of histone deacetylase 2 increases apoptosis and p21Cip1/WAF1 expression, independent of histone deacetylase 1. *Cell Death Differ* 2005;12:395–404.
16. Brodeur GM. Neuroblastoma: biological insights into a clinical enigma. *Nat Rev Cancer* 2003;3: 203–16.
17. Oberthuer A, Berthold F, Warnat P, et al. Customized oligonucleotide microarray gene expression-based classification of neuroblastoma patients outperforms current clinical risk stratification. *J Clin Oncol* 2006; 24:5070–8.
18. Berthold F, Hero B. Neuroblastoma: current drug therapy recommendations as part of the total treatment approach. *Drugs* 2000;59:1261–77.
19. Berthold F, Hero B, Kremens B, et al. Long-term results and risk profiles of patients in five consecutive trials (1979–1997) with stage 4 neuroblastoma over 1 year of age. *Cancer Lett* 2003;197:11–7.
20. Brodeur GM, Pritchard J, Berthold F, et al. Revisions of the international criteria for neuroblastoma diagnosis, staging, and response to treatment. *J Clin Oncol* 1993;11:1466–77.
21. Shimada H, Chatten J, Newton WA, Jr., et al. Histopathologic prognostic factors in neuroblastic tumors: definition of subtypes of ganglioneuroblastoma and an age-linked classification of neuroblastomas. *J Natl Cancer Inst* 1984;73:405–16.
22. Shimada H, Ambros IM, Dehner LP, et al. The International Neuroblastoma Pathology Classification (the Shimada system). *Cancer* 1999;86:364–72.
23. Spitz R, Hero B, Westermann F, Ernestus K, Schwab M, Berthold F. Fluorescence *in situ* hybridization analyses of chromosome band 1p36 in neuroblastoma detect two classes of alterations. *Genes Chromosomes Cancer* 2002;34:299–305.
24. Spitz R, Hero B, Ernestus K, Berthold F. Deletions in chromosome arms 3p and 11q are new prognostic markers in localized and 4s neuroblastoma. *Clin Cancer Res* 2003;9:52–8.
25. Fischer M, Skowron M, Berthold F. Reliable transcript quantification by real-time reverse transcriptase-polymerase chain reaction in primary neuroblastoma using normalization to averaged expression levels of the control genes *HPRT1* and *SDHA*. *J Mol Diagn* 2005;7:89–96.
26. Witt O, Monkemeyer S, Ronndahl G, et al. Induction of fetal hemoglobin expression by the histone deacetylase inhibitor apicidin. *Blood* 2003;101:2001–7.
27. Hothorn T, Lausen B. Maximally selected rank statistics in R. *R News* 2002;2:3–5.
28. Deubzer HE, Ehemann V, Kulozik AE, et al. Antineuroblastoma activity of *Helminthosporium carbonum* (HC)-toxin is superior to that of other differentiating compounds *in vitro*. *Cancer Lett* 2008; 264:21–28.
29. Waltregny D, Glenisson W, Tran SL, et al. Histone deacetylase HDAC8 associates with smooth muscle α -actin and is essential for smooth muscle cell contractility. *FASEB J* 2005;19:966–8.
30. Oehme I, Bosser S, Zornig M. Agonists of an ecdysone-inducible mammalian expression system inhibit Fas ligand- and TRAIL-induced apoptosis in the human colon carcinoma cell line RKO. *Cell Death Differ* 2006;13:189–201.
31. Ehemann V, Sykora J, Vera-Delgado J, Lange A, Otto HF. Flow cytometric detection of spontaneous apoptosis in human breast cancer using the TUNEL-technique. *Cancer Lett* 2003;194:125–31.
32. Deubzer HE, Ehemann V, Westermann F, et al. Histone deacetylase inhibitor *Helminthosporium carbonum* (HC)-toxin suppresses the malignant phenotype of neuroblastoma cells. *Int J Cancer* 2008;122: 1891–900.
33. Wegener D, Wirsching F, Riestler D, Schwienhorst A. A fluorogenic histone deacetylase assay well suited for high-throughput activity screening. *Chem Biol* 2003;10:61–8.
34. Shimada H, Umehara S, Monobe Y, et al. International neuroblastoma pathology classification for prognostic evaluation of patients with peripheral neuroblastic tumors: a report from the Children's Cancer Group. *Cancer* 2001;92:2451–61.
35. Walton JD, Kattan DR, Thomas SK, et al. Characteristics of stem cells from human neuroblastoma cell lines and in tumors. *Neoplasia* 2004;6:838–45.
36. Richon VM, Sandhoff TW, Rifkind RA, Marks PA. Histone deacetylase inhibitor selectively induces p21WAF1 expression and gene-associated histone acetylation. *Proc Natl Acad Sci U S A* 2000;97: 10014–9.
37. Hubbert C, Guardiola A, Shao R, et al. HDAC6 is a microtubule-associated deacetylase. *Nature* 2002; 417:455–8.
38. Waltregny D, De Leval L, Glenisson W, et al. Expression of histone deacetylase 8, a class I histone deacetylase, is restricted to cells showing smooth muscle differentiation in normal human tissues. *Am J Pathol* 2004;165:553–64.
39. Vannini A, Volpari C, Filocamo G, et al. Crystal structure of a eukaryotic zinc-dependent histone deacetylase, human HDAC8, complexed with a hydroxamic acid inhibitor. *Proc Natl Acad Sci U S A* 2004;101: 15064–9.
40. Lee H, Sengupta N, Villagra A, Rezai-Zadeh N, Seto E. Histone deacetylase 8 safeguards the human ever-shorter telomeres 1B (hEST1B) protein from ubiquitin-mediated degradation. *Mol Cell Biol* 2006; 26:5259–69.
41. Choi JH, Kwon HJ, Yoon BI, et al. Expression profile of histone deacetylase 1 in gastric cancer tissues. *Jpn J Cancer Res* 2001;92:1300–4.
42. Wilson AJ, Byun DS, Popova N, et al. Histone deacetylase 3 (HDAC3) and other class I HDACs regulate colon cell maturation and p21 expression and are deregulated in human colon cancer. *J Biol Chem* 2006;281:13548–58.
43. Zhang Z, Yamashita H, Toyama T, et al. Quantitation of HDAC1 mRNA expression in invasive carcinoma of the breast*. *Breast Cancer Res Treat* 2005;94:11–6.
44. Keshelava N, Davicioni E, Wan Z, et al. Histone deacetylase 1 gene expression and sensitization of multidrug-resistant neuroblastoma cell lines to cytotoxic agents by decapeptide. *J Natl Cancer Inst* 2007;99:1107–19.

Acknowledgments

We thank H. Christiansen (Pediatric Oncology, University of Marburg, Marburg, Germany) and M. Schwab (Division of Tumor Genetics, German Cancer Research Center, Heidelberg, Germany) for the analysis of *N-myc* amplification status of tumor samples of the German Neuroblastoma trials; R. Spitz (Pediatric Oncology, University of Cologne, Cologne, Germany) for the aforementioned analysis and 1p and 11q status analysis; Angelika Knüppel for her excellent technical assistance; and Gabriele Becker for her skillful technical support in flow cytometry.